◆ Human Brain Mapping 38:5890–5904 (2017) ◆

Gray Matter Asymmetries in Aging and Neurodegeneration: A Review and Meta-Analysis

Lora Minkova,[1,2,3]* **Annegret Habich**,[1,2,4] **Jessica Peter**,[1,2,4] **Christoph P. Kaller**,[2,5,6] **Simon B. Eickhoff**,[7,8] **and Stefan Klöppel**[1,2,4,9]

[1]*Department of Psychiatry and Psychotherapy, Faculty of Medicine, University of Freiburg, Freiburg, Germany*
[2]*Freiburg Brain Imaging Center, Faculty of Medicine, University of Freiburg, Freiburg, Germany*
[3]*Laboratory for Biological and Personality Psychology, Department of Psychology, University of Freiburg, Freiburg, Germany*
[4]*University Hospital of Old Age Psychiatry and Psychotherapy, University of Bern, Bern, Switzerland*
[5]*Department of Neurology, Faculty of Medicine, University of Freiburg, Freiburg, Germany*
[6]*BrainLinks-BrainTools Cluster of Excellence, University of Freiburg, Freiburg, Germany*
[7]*Institute of Systems Neuroscience, Medical Faculty, Heinrich-Heine-University, Düsseldorf, Germany*
[8]*Institute of Neuroscience and Medicine (INM-7) Research Centre Jülich, Jülich, Germany*
[9]*Center for Geriatric Medicine and Gerontology, Faculty of Medicine, University of Freiburg, Freiburg, Germany*

Abstract: Inter-hemispheric asymmetries are a common phenomenon of the human brain. Some evidence suggests that neurodegeneration related to aging and disease may preferentially affect the left—usually language- and motor-dominant—hemisphere. Here, we used activation likelihood estimation meta-analysis to assess gray matter (GM) loss and its lateralization in healthy aging and in neurodegeneration, namely, mild cognitive impairment (MCI), Alzheimer's dementia (AD), Parkinson's disease (PD), and Huntington's disease (HD). This meta-analysis, comprising 159 voxel-based morphometry publications (enrolling 4,469 patients and 4,307 controls), revealed that GM decline appeared to be asymmetric at trend levels but provided no evidence for increased left-hemisphere vulnerability. Regions with asymmetric GM decline were located in areas primarily affected by neurodegeneration. In HD, the left putamen showed converging evidence for more pronounced atrophy, while no consistent pattern was found in PD. In MCI, the right hippocampus was more atrophic than its left counterpart, a pattern that reversed in AD. The stability of these findings was confirmed using permutation tests. However, due to the lenient threshold used in the asymmetry analysis, further work is needed to confirm our results and to provide a better understanding of the functional role of GM asymmetries, for instance in the context of cognitive reserve and compensation. *Hum Brain Mapp 38:5890–5904, 2017.*

Additional Supporting Information may be found in the online version of this article.

Contract grant sponsor: CHDI/high Q Foundation Inc

*Correspondence to: Lora Minkova, Department of Psychiatry and Psychotherapy, Faculty of Medicine, University of Freiburg, Freiburg Brain Imaging, Breisacher Str. 64, 79106 Freiburg, Germany. E-mail: lora.minkova@uniklinik-freiburg.de

Received for publication 16 December 2016; Revised 3 August 2017; Accepted 20 August 2017.

DOI: 10.1002/hbm.23772

Published online 30 August 2017 in Wiley Online Library (wileyonlinelibrary.com).

Key words: VBM; ALE; aging; dementia; Parkinson's disease; Huntington's disease

INTRODUCTION

Asymmetries of brain function and structure are a common phenomenon in both humans and animals including non-human primates [Toga and Thompson, 2003], which is most likely arising from a complex interplay of genetic and environmental factors. Neurodegeneration, either associated with normal aging or diseases such as Huntington's disease (HD), Parkinson's disease (PD), and Alzheimer's dementia (AD), may interact with existing asymmetries or exacerbate them [Toga and Thompson, 2003]. In particular, there is evidence that the left hemisphere may be predominantly affected in all of the aforementioned pathological conditions. This includes a trend for faster gray matter (GM) loss of the left prefrontal cortex relative to the right one in healthy aging [Thompson et al., 2003]—a finding that was not consistently reported in all previous studies [e.g., Raz et al., 1997]. Longitudinal data indicate faster left-hemisphere cortical degeneration in AD [Thompson et al., 2001, 2003], and to a lesser extent in the pre-dementia stage, termed mild cognitive impairment (MCI) [Derflinger et al., 2011]. Faster left-hemisphere degeneration is correlated with worse performance in language-based neuropsychological tests across MCI and AD [Derflinger et al., 2011]. Lateralization of pathological GM changes has also been reported in HD, a hereditary neurodegenerative disorder that can be diagnozed with certainty decades before symptom onset. Specifically, stronger atrophy in the left striatum has been found in the pre-symptomatic [Lambrecq et al., 2013] and in one study also in the manifest stage of HD [Mühlau et al., 2007].

However, the nature of this suggested left-hemisphere dominance of degeneration across different conditions remains unclear. One potential explanation could be provided by the dominant role of that hemisphere (e.g., language function and the control of the dominant hand in right-handers), leading to increased neuronal activity that might be detrimental, causing a "burnout" through excitotoxicity or other mechanisms [Jagust, 2009]. On the other hand, relatively few studies have explicitly investigated inter-hemispheric differences in atrophy and substantial discrepancies exist between reports. In addition, the left-dominant reduction in GM volume seems to spread across different cortical and subcortical regions and is not restricted to the most clearly lateralized systems, i.e., motor or language. Finally, part of the presumably increased left-hemisphere vulnerability could also be explained by a detection bias, since a dysfunctional left hemisphere induces symptoms that are clinically more salient (e.g., language, verbal episodic memory) and hence over-represented in diagnostic criteria. For example, individuals with smaller left than right hemispheric volumes are more likely to report cognitive deficits or be diagnosed with MCI [Cherbuin et al., 2010].

Here, we aimed to investigate whether there was indeed consistent evidence for increased vulnerability of the left brain hemisphere across aging and neurodegeneration. To aggregate available data, we conducted a coordinate-based meta-analysis of previously published whole-brain voxel-based morphometry (VBM) studies on GM reduction in healthy aging, MCI, AD, PD, and HD using the well-established activation likelihood estimation (ALE) approach [Eickhoff et al., 2009, 2012]. Specifically, we assessed hemisphere asymmetries in GM atrophy for each group separately by performing the ALE analysis for all reported foci as well as for their left–right reversed versions and computing the voxel-wise differences between the corresponding ALE maps. Additionally, lobar asymmetries were investigated using a region-of-interest (ROI)-based ALE analysis assessing the per-voxel probabilities of all reported foci, i.e., the presumed hotspots of atrophy, per lobe and hemisphere.

Finally, to address the functional role of the seed regions found in the GM asymmetry analysis, we analyzed their functional profiles based on behavioral domains (i.e., the mental operations isolated by the experiments that co-activated with each seed) and paradigm classes (i.e., the experimental tasks used in the respective experiments). Furthermore, we sought to examine their patterns of task-based co-activation with the rest of the brain by using meta-analytic connectivity modeling (MACM). We hypothesized that regions showing GM asymmetry would also show differential co-activation pattern, possibly influenced by topologically selective changes in the brain.

Abbreviations

AD	Alzheimer's dementia;
ALE	activation likelihood estimation;
BD	behavioral domain;
HC	healthy controls;
(pre-)HD	(preclinical) Huntington's disease;
GM	gray matter;
MA	modeled activation;
MACM	meta-analytic connectivity analysis;
MCI	mild cognitive impairment;
PC	paradigm class;
PD	Parkinson's disease;
VBM	voxel-based morphometry.

MATERIALS AND METHODS

Data Source

A comprehensive systematic search was conducted in the PubMed (http://ncbi.nlm.nih.gov/pubmed) and BrainMap

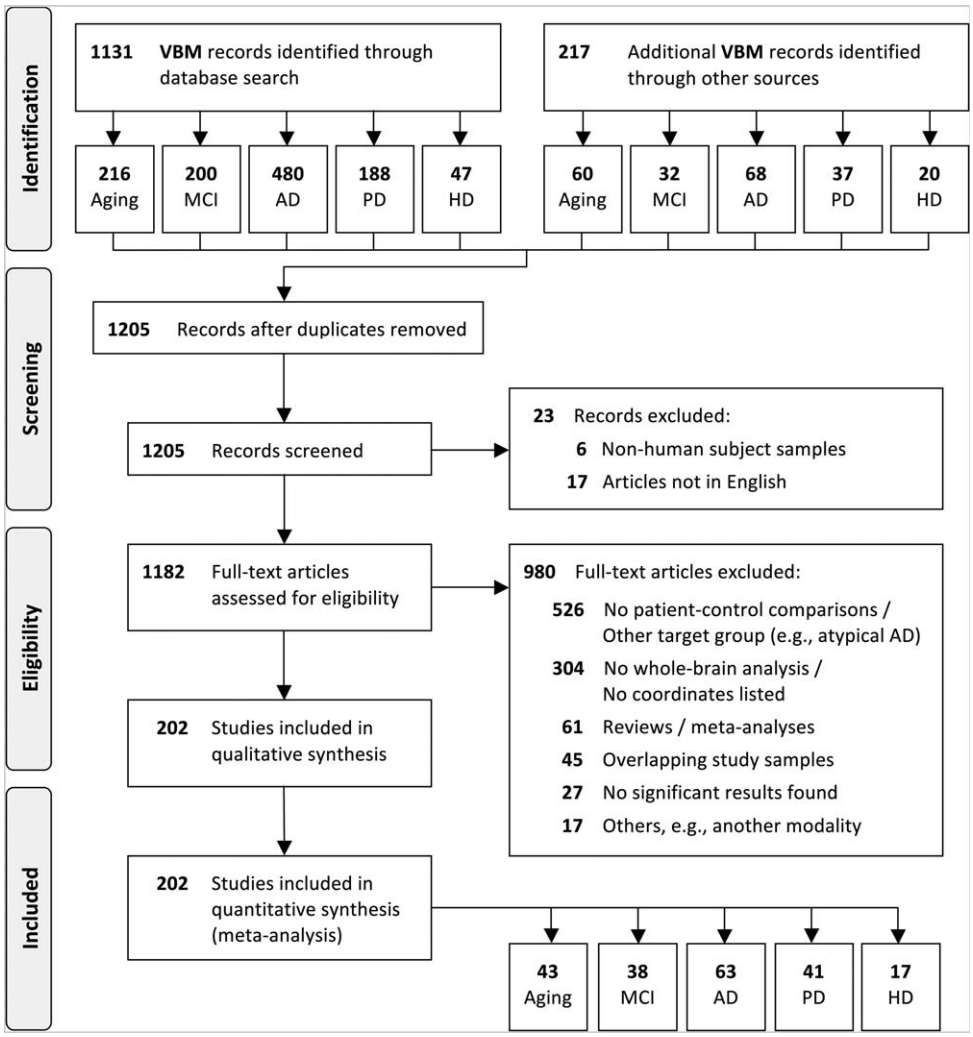

Figure 1.
PRISMA flow diagram of study selection.

(http://brainmap.org) [Fox et al., 2005; Fox and Lancaster, 2002; Laird et al., 2005b, 2009, 2011) databases from January 1991 until February 2016 to identify VBM articles on whole-brain GM atrophy in healthy aging, MCI, AD, PD, and HD. The following keywords were used in appropriate combinations: "grey/gray matter," "voxel-based morphometry,", "VBM," "healthy aging," "aging," "ageing," "age effects," "mild cognitive impairment," "MCI," "Alzheimer's disease," "AD," "Parkinson's disease," "PD," "Huntington's disease," "HD."

Selection Criteria

The process of selecting eligible articles was performed according to the Preferred Reporting Items for Systematic Reviews and Meta-Analyses (PRISMA) statement [Moher et al., 2009]. The flow chart of the selection process is illustrated in Figure 1.

We first screened all identified publications and selected only those on humans published in peer-reviewed English language journals. Full-text articles were then assessed for eligibility and were selected if (1) a voxel-wise whole-brain analysis was performed, (2) coordinates were reported in a defined stereotaxic space (i.e., Talairach or Montreal Neurological Institute (MNI) space), and (3) comparisons between patients and matched healthy control participants were included, with the exception of studies in healthy aging, which had to include young and older healthy adults. Any articles that reported results only after small-volume correction within a region of interest were excluded from the meta-analysis. Publications that did not report any decline in GM were also excluded from the analysis. Of note, the ALE approach tests for the above-

chance convergence of results across different experiments and therefore cannot deal with experiments that do not report any significant result. The selection was furthermore restricted to publications on typical AD and PD, thus excluding those on other dementia and atypical Parkinson's syndromes. Reviews and meta-analyses were also excluded but their references were manually reviewed for inclusion of additional publications that might have been missed during the data search. Publications from the same authors and/or research group(s), as well as those using data from publicly available databases (e.g., ADNI, http://adni.loni.usc.edu), were closely inspected to ensure that the same study sample was included only once in the current meta-analysis. In case of overlapping samples between articles, only those with a bigger sample size and/or more detailed information reported (e.g., coordinates and demographic data) were included. All publications included in the current meta-analysis were performed according to the ethical standards recommended by the Helsinki Declaration [World Medical Association, 2013].

Data Extraction

Demographic and technical details were extracted from each article, including the first author's name, year of publication, study population and sample size, age, gender, handedness if reported, scanner magnetic field strength, image resolution, covariates, software and methods (e.g., algorithm, smoothing, thresholds, etc.) used for analysis (see Supporting Information Tables S1 and S2).

Coordinates of GM volume (or density) reduction were collected from each article and included in the meta-analysis. Separate contrasts (i.e., lists of foci) were created for each pair of patient–control comparison. If an article reported coordinates for multiple patient groups (e.g., MCI and AD) that were considered relevant for the current meta-analysis, each patient–control comparison was included as a separate contrast. To avoid ambiguities, we use the term "article" throughout the text to denote a publication and "experiment" to denote each contrast reported therein.

In case of healthy aging, we were interested in investigating the age-related effects on GM atrophy. Therefore, coordinates reported from either a group comparison (i.e., Old < Young) or a correlation analysis with age (i.e., decreasing GM volume/density with advancing age) were included, since the location of significant effects, rather than the actual statistical values, are pooled in an ALE meta-analysis. While limited data have indicated a possible increase in GM in aging [e.g., following aerobic fitness training; Colcombe et al., 2006], the current analyses focused only on GM decline, reflecting effects of neurodegeneration. Similarly, only GM decline in the patients relative to controls (but not vice versa) were investigated.

We aimed to be as inclusive as possible and extracted all coordinates that were reported as statistically significant at a threshold of $P < 0.05$ whole-brain corrected or $P < 0.005$ uncorrected with a cluster threshold. Those coordinates reported in Talairach space were converted into MNI space using Lancaster's tal2icbm transform [Laird et al., 2010; Lancaster et al., 2007]. Those reported in Talairach space obtained using the old Brett transform (mni2tal) were converted back into MNI by applying the inverse of the Brett transform (tal2mni).

ALE Meta-Analysis

The ALE technique is a well-established data-driven meta-analytic approach used to test for above-chance convergence of peak coordinates (i.e., foci) reported across individual experiments [Laird et al., 2005a; Turkeltaub et al., 2002]. Here, we used a revised version of the ALE algorithm [Eickhoff et al., 2009, 2012], which treats foci as 3-dimensional Gaussian probability distributions centered at the given coordinates, rather than as single points. The width of the probability distribution is based on empirical estimates of the spatial uncertainty due to the between-subject or between-template variance associated with each single focus, thus resulting in a random-effects analysis. The between-subject variance is weighted by the sample size investigated in each experiment included, with larger sample sizes modeled by smaller Gaussian distributions and providing more reliable approximations of the "true" activation effect.

VBM-based ALE meta-analyses were conducted separately for each patient group (MCI, AD, HD, and PD) in order to identify disease-specific patterns of GM atrophies reported in the literature. Although most of the experiments included in the meta-analysis defined age as a covariate to correct for confounding effects, we also explicitly addressed age-related GM atrophies by conducting an additional ALE analysis in healthy aging.

The ALE meta-analyses were performed using in-house MATLAB scripts. First, the probability distributions of all foci within a given experiment were combined for each voxel, resulting in modeled activation (MA) maps, which indicated the probability at each location that a significant difference was located at that position [Turkeltaub et al., 2002]. Then, the union of all these MA maps were calculated to determine the voxel-wise ALE scores, which quantified the convergence of results across different experiments. To assess whether the convergence of foci was true or merely the result of random noise, the ALE scores were compared with the empirical null distribution, reflecting the random spatial association between experiments with a fixed within-experiment distribution of foci [Eickhoff et al, 2012; cf. Goodkind et al., 2015].

Finally, as recommended by a recent simulation study [Eickhoff et al., 2016], the resulting *P*-values were thresholded at $P < 0.05$, cluster-level family-wise error (cFWE)

corrected (cluster-forming threshold at voxel-level $P < 0.001$) and transformed into Z-scores for display. The resulting brain areas were anatomically labeled according to the probabilistic cytoarchitectonic maps of the SPM Anatomy toolbox v.2.1 [Eickhoff et al., 2005, 2006, 2007] and visualized using the MRIcron software (https://www.nitrc.org/projects/mricron).

Asymmetry meta-analysis

To assess the hemispheric asymmetries in GM atrophy reported in the literature, we left–right reversed the locations extracted from each experiment by multiplying the x-coordinates of each foci by -1. A subtraction analysis [Eickhoff et al., 2011] between the original and the flipped foci was then performed to compute the voxel-wise difference between the two ALE maps, respectively. This was achieved by performing ALE separately for the original and the flipped foci and computing the voxel-wise difference between the ensuing ALE maps.

Permutations were used to test the significance of the results by pooling all experiments contributing to either analysis alone and randomly dividing them into two groups of the same size as the two original sets. This process was repeated 50,000 times, yielding a voxel-wise null distribution on the differences in ALE scores between the two sub-analyses. The true differences in ALE scores were then tested against the null hypothesis of label exchangeability and thresholded at a posterior probability of $P > 0.95$ for true differences (cFWE-corrected, with a cluster-defining threshold of $P = 0.05$ unc.). Finally, the voxel-wise P-value images were converted to Z-scores for display and masked by the respective main effects (i.e., the significant effects in the ALE for original and flipped foci).

Additionally, global inter-hemispheric asymmetries were assessed using a ROI-based ALE analysis for each lobe and hemisphere, which can handle the spatial uncertainty of the reported foci. ROIs were based on the LONI Probabilistic Brain Atlas [LPBA40; Shattuck et al., 2008] and comprised the following areas per hemisphere: frontal, temporal, parietal, occipital, insular, cingulum, cerebellum, and sub-cortical areas. Statistical significance was defined at a threshold of $P < 0.003$ (Bonferroni-corrected for the number of ROIs = 16, or 8 per hemisphere).

Functional characterization

To describe the functional role of the seed regions identified by the asymmetry analysis, their functional profiles were assessed using the behavioral domain and paradigm class meta-data stored for each experiment in the BrainMap database. Additionally, we repeated the functional decoding analysis using the seeds' flipped versions in order to capture potential inter-hemispheric differences in their functional profiles.

A reverse inference approach was used to determine the most likely above-chance taxonomic associations for each seed of interest [cf. Bzdok et al., 2013]. Behavioral domains (BDs), denoting the mental processes isolated by each experiment, can consist of the following main categories (each including several sub-categories): cognition, action, perception, emotion, and interoception [Fox et al., 2005; Lancaster et al., 2012]. Paradigm classes (PCs), on the other hand, describe the specific experimental conditions/contrasts employed [e.g., finger tapping, emotional face recognition, etc.; see Turner and Laird, 2012]. The reverse inference approach determines the probability of a BD given an activation in a particular cluster, i.e., P(Domain | Activation), as well as the probability of a PC for a given seed, i.e., P(Paradigm | Activation), that is higher than the global BDs and PCs of all the articles in the BrainMap database. The statistical significance of the functional profiles was tested using a binomial test ($P < 0.05$, Bonferroni-corrected for multiple comparisons).

Task-based co-activation analysis

MACM [Eickhoff et al., 2010] was applied to assess the functional connectivity of regions identified in the asymmetry analysis. MACM is a data-driven method that can be used to identify connections within an indirect network by determining the brain areas that co-activate with a given seed region at above-chance level across many neuroimaging experiments [Fox et al., 2014].

Briefly, Sleuth 2.4 (http://brainmap.org/sleuth/) [Fox et al., 2005; Fox and Lancaster, 2002; Laird et al., 2005b, 2009, 2011] was used to search the BrainMap database for all neuroimaging experiments that activated each seed region, as well as their flipped versions. The search was restricted to articles using functional magnetic resonance imaging (fMRI) and positron emission tomography (PET) in healthy adults (i.e., no interventions and no group comparisons) with coordinates reported in stereotaxic space, which yielded 9,331 eligible experiments at the time of analysis (April 2016). After identifying the relevant experiments for each (original or flipped) seed separately, ALE meta-analyses were performed to test for convergence across the foci reported in these experiments. Significant convergence outside the seed regions was defined at a threshold of $P < 0.05$ after cFWE correction, as described above, and indicated consistent co-activation with the respective seed region. Additionally, we assessed the differential and converging co-activation patterns between each pair of original and flipped seeds using contrast and minimum statistic conjunction analyses, respectively, with the ensuing MACM maps.

RESULTS

Sample Characteristics

The sample characteristics are summarized in Table I. Detailed demographic and technical information is provided in Supporting Information Tables A1 and A2.

TABLE I. Sample characteristics

	Aging	MCI	AD	PD	HD
No. of experiments	43	40	63	42	18
No. of subjects	4,195	828	1,430	908	541
Age (mean ± SD, years) (range[a])	53.4 ± 12.9 (18–95)	71.4 ± 3.0 (46–85)	71.4 ± 4.3 (46–95)	65.9 ± 4.9 (27–88)	45.2 ± 5.5 (19–68)
Gender (Female, %)	53.6%	54.9%	55.2%	40.7%	64.7%
Handedness[a] (Right, %)	91.7%	100.0%	94.4%	97.0%	87.9%

[a]Handedness and age range were not reported in all experiments (see Supporting Information Table S2 for more details).
Abbreviations: MCI = mild cognitive impairment, AD = Alzheimer's dementia, PD = Parkinson's disease, HD = Huntington's disease.

Our initial search identified 1,348 publications, from which a total of 202 articles fulfilled the inclusion criteria (Fig. 1). Out of them, 43 reported age-related effects, including 4,195 healthy adults with an age range between 18 and 86 years. The remaining 159 articles reported comparisons between 4,469 patients and 4,307 healthy matched controls, comprising a total of 163 experiments (i.e., patient–control comparisons). No analyses were performed between manifest and pre-symptomatic HD, neither between PD with versus without cognitive deficits, due to the small number of eligible experiments (preHD: 4 reports with 170 individuals; PD with cognitive deficits: 7 reports with 102 patients), which is not sufficient for reliable ALE analyses [Eickhoff et al., 2016].

VBM-ALE Results

Figure 2 illustrates the patterns of regional GM loss in red and their hemispheric asymmetries in blue, revealed by the ALE meta-analysis in (Fig. 2A) healthy aging, (Fig. 2B) MCI, (Fig. 2C) AD, and (Fig. 2D) HD ($P < 0.05$, cFWE-corrected, with a cluster-defining threshold of $P = 0.001$). The ALE analysis did not show any significant differences between PD and controls ($P < 0.1$, cFWE-corrected), irrespective whether studies in PD with cognitive deficits were included or not. Asymmetry in GM loss was found only in aging, with converging evidence for a stronger leftward-biased asymmetry in the supramarginal gyrus. In additional post hoc exploratory analysis, the asymmetry analysis was repeated with a more liberal cluster-defining threshold of $P = 0.05$. Subsequently, the resulting clusters were cFWE corrected at $P = 0.05$. The corresponding coordinates are listed in the Supporting Information: Table S3 for GM loss and Table S4 for the asymmetries in GM loss.

In healthy aging, regional GM loss was found in the insular cortex, prefrontal regions, including the inferior and middle prefrontal gyri, as well as in the postcentral gyrus within the somatosensory association cortex. However, we did not find any consistent evidence for lateralization of GM loss in frontal regions. Instead, stronger GM loss was present in the postcentral gyrus in the left relative to the right hemisphere, while GM loss in the superior temporal gyrus was evident on the right side.

In MCI, the ALE meta-analysis revealed bilateral GM loss in the hippocampus compared to controls. Experiments more consistently reported smaller right than left hippocampus. However, this pattern reversed in AD, where we found more evidence for bilateral but still stronger leftward-biased hippocampal GM loss, while rightward-biased atrophies were more consistently found in a cluster comprising the superior and middle temporal gyri. Other regions showing bilateral GM loss in AD included the left anterior insula and thalamus. If MCI and AD were combined together as one group, the results suggested again a bilateral GM loss in the hippocampus, with some converging evidence for a left-biased asymmetry, possibly driven by the bigger AD sample compared to the MCI one. Finally, in HD mutation gene carriers, there was a bilateral decrease in striatal GM compared to healthy controls, with converging evidence for a stronger leftward-biased asymmetry in the putamen.

The additional ROI-based ALE analysis did not reveal any effects of global lobar lateralization (all raw $P > 0.1$). Figure 3 illustrates the probabilistic number of "true" foci locations of decreased GM within each lobe and hemisphere. In aging, most foci were located in the frontal lobe, with less locations reported for the parietal and temporal lobes. In MCI, most foci were located in the temporal lobe, followed by the frontal lobe and subcortical regions, including the hippocampus. In AD, in addition to temporal, frontal, and subcortical regions, GM loss was also increasingly reported in the parietal lobe. In HD, most foci were located in the frontal and subcortical regions, followed by the parietal and occipital lobes. Finally, GM loss in PD was reported for the frontal lobe but, interestingly, less so for subcortical regions.

Functional profiles

Using functional decoding, we intended to link the brain regions that were topologically defined by the ALE asymmetry analysis to their corresponding mental processes. The analysis included the following ROIs (Fig. 2, Supporting Information Table S4): left supramarginal and right superior temporal gyri (asymmetric GM identified in aging), right hippocampus (MCI), left hippocampus and right superior temporal gyrus (AD), and left putamen (found in HD). Additionally, the seeds' flipped versions

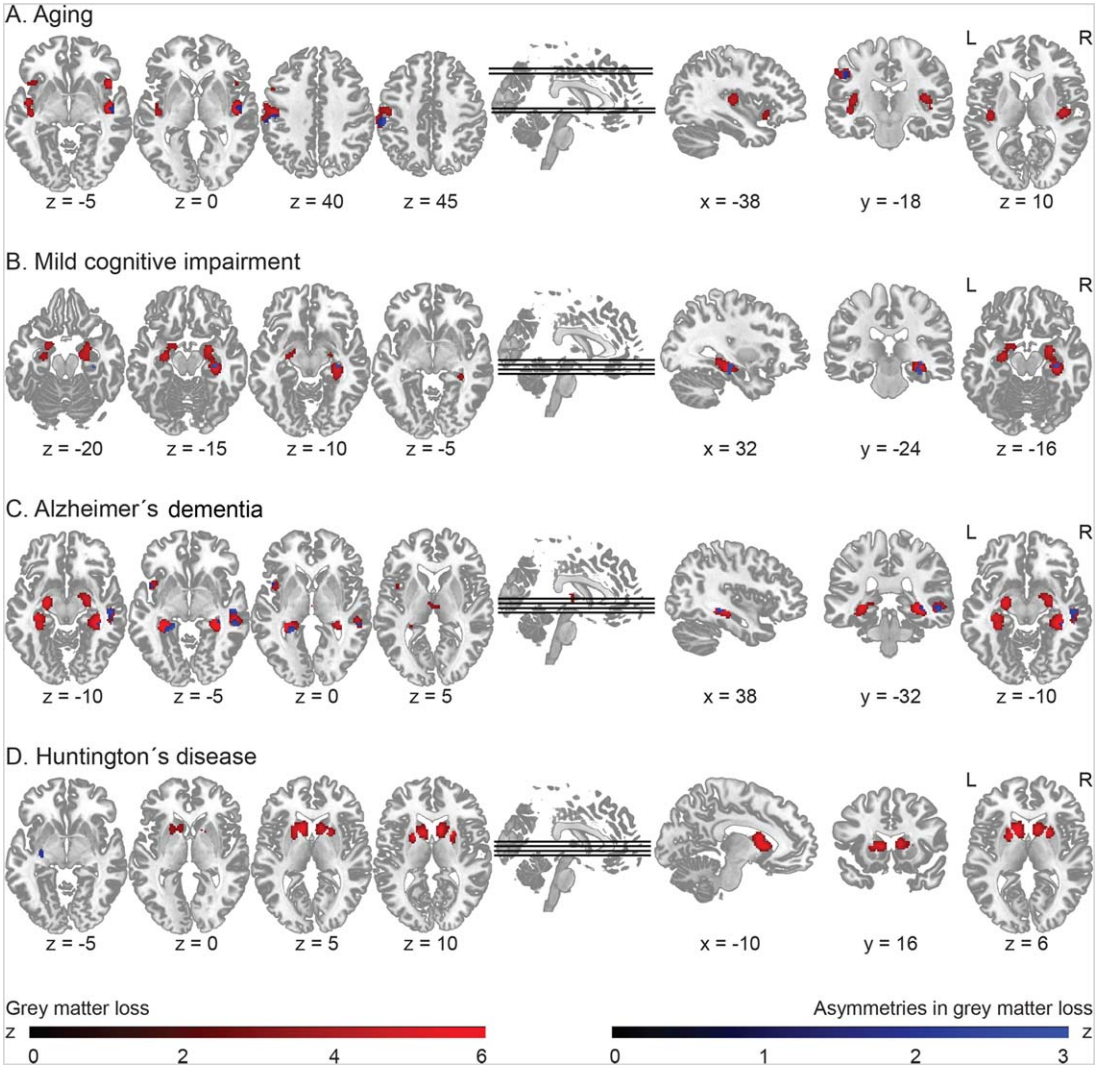

Figure 2.

ALE results: Patterns of gray matter decline (in red) and asymmetries in gray matter decline (in blue), separately in healthy aging (**A**), MCI (**B**), AD (**C**), and HD. Coordinates [*x*/*y*/*z*] are provided in MNI space. L indicates left and R indicates right. [Color figure can be viewed at wileyonlinelibrary.com]

were also analyzed in order to account for potential interhemispheric differences in functional profiles. Please note that only the supramarginal gyrus survived the initial correction for multiple comparisons, while the other peaks were identified at a more lenient cluster-defining threshold and the reported results should therefore be considered with caution.

The supramarginal gyrus and its flipped (i.e., right) version were associated with BDs on action (execution; $z = 6.38$ and $z = 4.22$, $P < 0.05$, for left and right hemispheres, respectively), while only the left seed was also linked to perception (somesthesis; $z = 4.92$, $P < 0.05$). PCs recruiting these areas included finger tapping (both hemispheres; $z_{left} = 4.41$, $z_{right} = 3.05$, $P < 0.05$), as well as flexion-extension ($z = 4.07$, $P < 0.05$) and vibrotactile monitor discrimination tasks: $z = 4.08$, $P < 0.05$ (left hemisphere only). The right superior temporal gyrus was linked to cognition only (language phonology; $z = 3.21$, $P < 0.05$), while its' left flipped version involved BDs on cognition (language: phonology ($z = 3.56$), speech ($z = 4.67$), and music ($z = 3.31$)), as well as on perception (audition; $z = 6.60$). The following PCs were involved: pitch ($z_{left} = 4.82$, $z_{right} = 4.04$) and phonological monitor discrimination tasks, $z_{left} = 6.24$, $z_{right} = 4.41$ (both hemispheres), as well as passive listening: $z_{left} = 8.05$, drawing: $z_{left} = 5.16$, and overt reading: $z_{left} = 4.24$ (left hemisphere only).

The right and left hippocampi, which were found in the asymmetry analysis in MCI and AD respectively, were associated with the memory (explicit) BD (MCI: $z_{left} = 3.12$,

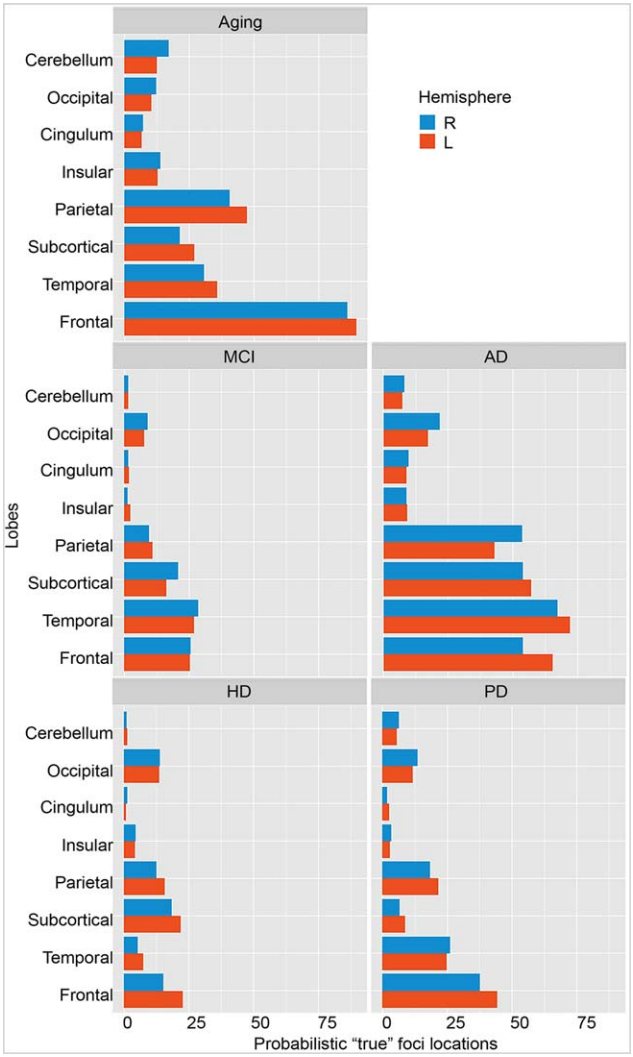

Figure 3.

ROI-based ALE: Probabilistic "true" foci locations across lobes and hemispheres. L indicates left and R indicates right. MCI = mild cognitive impairment; AD = Alzheimer's dementia, HD = Huntington's disease. [Color figure can be viewed at wileyonlinelibrary.com]

$z_{right} = 3.16$, and AD: $z_{left} = 3.58$, $z_{right} = 3.16$) and activated in experimental contrasts on encoding (MCI: $z_{left} = 3.34$, $z_{right} = 3.36$, and AD: $z_{left} = 3.23$, $z_{right} = 3.10$). The right superior temporal gyrus (found in AD) was associated with the perception (audition; $z = 8.64$) and cognition (music; $z = 4.14$) BDs and was involved in tasks on passive listening ($z = 8.05$) and music comprehension ($z = 6.64$). In addition, the left (i.e., flipped) superior temporal gyrus was associated with language (speech, syntax, semantics, and phonology: $z = 3.66$, $P < 0.05$) and was activated by the following experimental contrasts: word generation ($z = 3.39$), semantic ($z = 6.64$), and phonological discrimination ($z = 4.42$), and reading ($z = 4.25$).

Finally, the putamen was associated with BDs on action (left hemisphere only: $z_{left} = 3.46$) and emotion (both hemispheres: $z_{left} = 3.42$, $z_{right} = 4.74$). The experimental tasks included: finger tapping ($z_{left} = 3.39$), reward ($z_{left} = 3.53$), and face monitor discrimination ($z_{left} = 4.52$, $z_{right} = 3.06$).

Task-based co-activation results

In the MACM analysis, we sought to examine how the regions identified in the asymmetry analysis co-activate with the rest of the healthy brain based on data available in the BrainMap database in order to characterize their task-based functional connectivity patterns. The analysis was performed separately for each seed ROI, as well as for their flipped versions, and the results are illustrated in Figure 4 (for the corresponding coordinates, see Supporting Information Table S5). Significant convergence outside a seed indicates regions that are reliably coactivated with the respective seed.

Generally, all seed ROIs co-activated their homologues (i.e., the same region but in the opposite hemisphere), as shown in Figure 4. Surprisingly, we found widespread co-activation patterns only for two regions: the supramarginal gyrus found in aging and the superior temporal gyrus identified in AD. The supramarginal gyrus co-activated brain areas typically involved in executive and visuospatial tasks, including bilateral inferior frontal gyri, supplementary motor area (SMA), left thalamus, and left precentral gyrus. The superior temporal gyrus co-activated the left inferior frontal gyrus, left middle temporal gyrus, and the SMA.

No co-activations were found for the right hippocampus found in MCI, while the left hippocampal seed, identified in AD, co-activated the SMA. Finally, the left putamen, which showed asymmetric GM decline in HD, co-activated the left inferior frontal gyrus, left thalamus, and right amygdala.

DISCUSSION

Knowledge about the patterns of GM loss may provide valuable insights into the pathomechanisms associated with aging and neurodegeneration and thus prove useful for the development of future interventions as well as for studying cognitive reserve and compensation. In the present voxel-based quantitative meta-analysis, we aimed to analyze the patterns in asymmetries of volumetric GM changes associated with aging and various neurodegenerative diseases. By applying the ALE approach, our results illustrated the most representative structural changes that were consistently reported across a large body of VBM-based whole-brain studies, overcoming potential disadvantages of small sample sizes [cf. Goodkind et al., 2015; Eickhoff and Etkin, 2016].

The findings presented here do not confirm the hypothesized higher vulnerability of the left hemisphere but rather

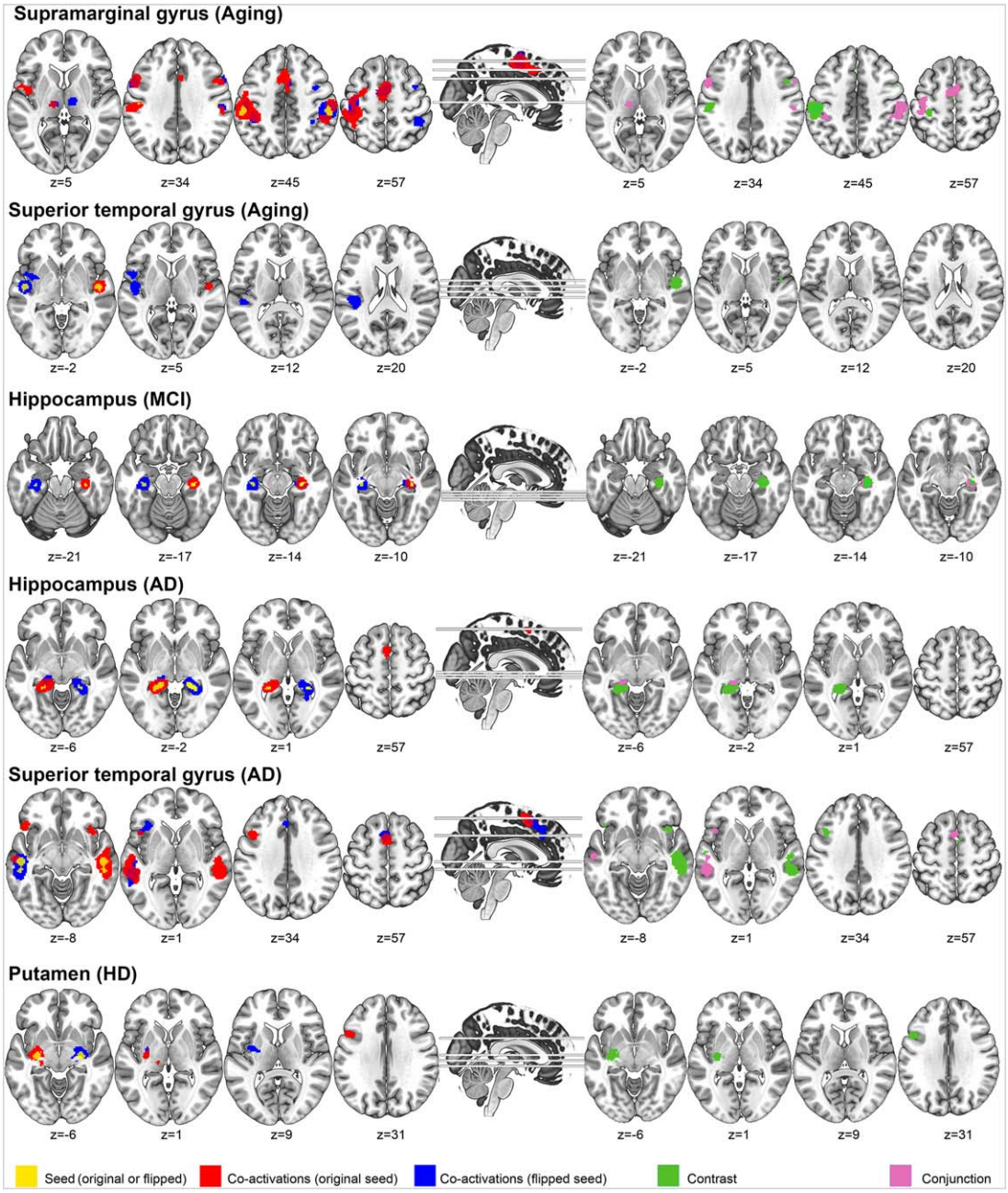

Figure 4.

MACM results for regions showing GM asymmetries. Yellow: seed regions used for each analysis. Red: co-activation patterns with the original seed. Blue: co-activation patterns with the flipped, contralateral seed. Green: Contrast/difference between original and flipped MACM results. Purple: Conjunction (minimum statistic) analysis between original and flipped MACM results. Coordinates [*x*/*y*/*z*] are provided in MNI space. L indicates left and R indicates right. [Color figure can be viewed at wileyonlinelibrary.com]

demonstrated region-specific asymmetric patterns in both hemispheres that were present in healthy aging and in different neurodegenerative diseases. Of note, the analyses were limited to pre-selected neurodegenerative diseases, namely MCI, AD, PD, and HD, and did not include others, such as atypical AD or other motor diseases besides HD and PD. Additionally, in order to detect subtler differences in GM asymmetry, we used a liberal

cluster-defining threshold prior to the cFWE correction. Therefore, the asymmetry results should be taken with caution.

We found converging evidence in the literature for a more pronounced GM loss of the left supramarginal and right superior temporal gyri in aging, the right hippocampus in MCI, the left hippocampus and right superior temporal gyrus in AD, and the left putamen in HD, compared to their contra-lateral homologues. As detailed in the subsequent sections, the identified functional profiles of these regions were consistent with BDs known to be affected by the respective diseases. In the MACM analysis, we expected to observe different task-based co-activation patterns between regions showing GM symmetry and their flipped homologues. However, the results did not support our hypothesis. Instead, we found no structural–functional correspondence, which might have been caused by failed convergence of data, as discussed in more detail below. Therefore, our results regarding the functional role of GM asymmetry are inconclusive and warrant further investigation.

Before discussing the condition-specific results, we would like to raise some methodological considerations, which are important for the interpretation of our results. First, ROI seed definitions were based purely on topographical grounds and may thus fail to account for more fine-grained distinctions in more heterogeneous regions [e.g., for a discussion on differential involvement of subregions in the premotor and frontal cortices, see Cieslik et al., 2016; Genon et al., 2017]. Second, we performed an analysis of asymmetry and included VBM-studies that themselves did not aim to focus on asymmetry and therefore did not employ an image processing (e.g., symmetric template to ensure voxel-wise correspondence between the two hemisphere) established for analyses of asymmetry [Kurth et al., 2015]. Third, studies investigating structural and functional asymmetries should ideally include only right-handed participants or at least consider effects of handedness. However, we believe that this was not a major issue in our analysis, given that the majority of participants were right-handed (see Supporting Information Table S2).

Most importantly, the distinction between convergence (as investigated by ALE) and effect size, which cannot be addressed with this method, is essential when interpreting the results. Thus, if there is a widespread atrophy with variable peak locations between different experiments, it may fail to converge in an ALE analysis, which relies on summarized, coordinate-based rather than on image-based, raw data [Salimi-Khorshidi et al., 2009]. In other words, this could potentially lead to attenuation of effects across studies if the reported peak locations are not consistently overlapping (see Supporting Information Fig. S1). Furthermore, the foci included in the meta-analysis are derived from maxima and do not provide any information about the cluster size or spread. Consequently, the ALE approach would be more robust for sub-cortical areas, where clusters are not so widespread (e.g., the hippocampus or putamen), than for cortical areas. Ideally, these methodological considerations could be addressed by conducting an image-based mega-analysis, using the statistical maps from each study, which would be laborious and currently infeasible due to limited accessibility to such data.

Healthy Aging

Consistent with a previous ALE meta-analysis in aging [Di et al., 2014], we found converging evidence for GM reduction in the inferior and middle prefrontal gyri, the postcentral gyrus, including the supramarginal gyrus, as well as in the insular cortex. Similarly, as illustrated by our lobar asymmetry analysis (Fig. 3), most peaks reported in healthy aging were located in the frontal lobe bilaterally, followed by the prefrontal and temporal lobes, which fits well with the existing literature. However, our results did not confirm the presumed leftward asymmetry of GM loss in frontal brain regions [Thompson et al., 2003]. Of note, the apparent lack of a more widespread atrophy or asymmetry in the frontal and parietal regions in our meta-analysis may result from the nature of the ALE approach (see methodological considerations above, as well as Supporting Information Fig. S1).

The lack of GM loss in the limbic system or shift in asymmetries thereof are consistent with previous reports [e.g., Good et al., 2001; Grieve et al., 2005; Long et al., 2013], suggesting that neurodegeneration of these structures is linked to AD-specific changes but not to healthy aging. However, if a cluster of GM decline spreads to both hemispheres, reports of the local maxima would fail to capture such asymmetries. Thus, our results provided here illustrate the most robust findings in the available literature by overcoming small size considerations, although eventually failing to address more heterogeneous cortical changes.

The converging evidence for an asymmetric GM loss found in the left supramarginal gyrus and the right superior temporal gyrus warrants further discussion. Using the functional decoding analysis, we showed that the left supramarginal gyrus was associated with executive function and bodily perception. Additionally, the MACM results suggested a connectivity pattern with regions part of known executive and sensorimotor networks, including the inferior frontal cortex, the SMA, and the primary motor cortex. Given the generally left-hemisphere dominance of the motor/sensorimotor network, this raises the question whether structural and functional asymmetries in aging are linked together. Di et al. [2014] observed an association between GM reduction of the dorsolateral prefrontal cortex and functional hyper-activation of the region during task performance, potentially indicating a compensational role. It could be argued that age- and disease-related asymmetries in neuroanatomy may give rise to

similar functional changes, possibly representing compensatory mechanisms that support the maintenance of cognitive function and/or illustrating early pathology-related deficits [for a review, see Grady, 2012].

The converging evidence for a rightward asymmetry in GM loss of the superior temporal gyrus that we have reported here is more difficult to disambiguate. Previous data suggest age-related metabolic decreases in the middle and superior temporal cortex, albeit less pronounced than in frontal regions, which were related to white matter disturbances in the long association fronto-temporo-occipital fibers [Chetelat et al., 2013]. At the same time, hemispheric perfusion seems to be asymmetric in the superior temporal cortex, i.e., right higher than left [Baird et al., 1999]. The lack of apparent functional–structural relationship evident by our functional decoding and MACM analyses, which are in contrast to the superior temporal peak found in the asymmetry analysis in AD, might point to failed convergence of data resulting from a slightly different ROI positioning and/or an asymmetric pattern resulting merely from structural dislocations due to a shift in the GM–white matter boundary following loss of myelin.

MCI and AD

In AD we found converging data for rightward-biased asymmetries (i.e., less GM in the right hemisphere) in a cluster comprising the middle and superior temporal gyri. Functional profiles linked the cluster to BDs of action (speed execution), perception (audition), and cognition (social cognition, language syntax, speech semantics, and phonology) [for a review, see Hodges, 2006]. In terms of activation-based co-activations, the right superior temporal gyrus co-activated the bilateral inferior frontal gyrus, which are part of the functional executive control network [Smith et al., 2009], the insular cortex, within the salience functional network [Seeley et al., 2007], and involved cognitive flexibility, the fusiform gyrus, and the SM, the latter also known to be involved in inhibitory control [Nachev et al., 2008], a domain that is also affected in AD [e.g., Amieva et al., 2004].

Furthermore, we found some evidence for leftward-biased hippocampal GM loss in AD, which is consistent with previous findings [Thompson et al., 2003, 2007]. Of note, we found right-lateralized atrophy of the hippocampus in MCI. In contrast to Thompson et al. [2003, 2007], others have also reported more severe atrophy of the right hemisphere in the medial and lateral temporal cortex as well as the parietal cortex observed in both amnestic MCI and AD [Apostolova et al., 2007]. It can be suggested that these discrepancies in the literature may result from stage-specific effects. Across studies, different criteria for MCI and in particular for its subtypes (e.g., amnestic MCI) but also for AD and its severity stages have been used, explaining discrepant results also in apparently identical disease stage. In this regard, it should be noted that, during the study selection for the ALE meta-analysis, no distinction between possible and probable AD and the severity stages was made. Similarly, the diagnostic criteria for MCI were adopted from the respective studies thus increasing the variability in our data.

In a recent analysis, it was demonstrated that AD patients with predominant language deficits exhibited more left-lateralized amyloid-β burden and hypometabolism than patients with predominant visuospatial impairment and vice versa [Frings et al., 2015]. In another study, bilateral but stronger right-hemisphere decline in glucose metabolism in the superior temporal areas in AD was associated with more pronounced semantic memory deficits [Giffard et al., 2008].

Huntington's Disease

HD is typically characterized by selected vulnerability of the basal ganglia. Here, we found bilateral GM atrophy in the striatum, with stronger leftward asymmetry in the putamen, which conforms to previously reported findings [Mühlau et al., 2007]. The ROI-based ALE analysis did not show any global hemispheric asymmetries across the lobes. Peaks were reported in the experiments for regions within the parietal, frontal, and occipital lobes bilaterally, all areas that are targeted by HD after disease manifestation. However, we found converging results for a GM lateralization across the studies only for the left putamen. Furthermore, the functional role of the left putamen involved mental processes of action (executive function) and emotion (fear and other). Thus, the seed was activated by tasks involving emotional face discrimination, reward, and finger tapping paradigms. This conforms to known clinical features of HD, characterized by deficits during finger tapping tasks [e.g., Klöppel et al., 2009], as well as in emotional processing [for a review, see Henley et al., 2012]. Of note, we were unable to answer the question whether these changes vary across the different stages of the disease (i.e., pre-symptomatic vs. manifest HD) due to the limited number of studies that reported findings in pre-HD individuals. Thus, the current meta-analysis was based on all studies that included HD mutation gene-carriers, irrespective of symptom manifestation. Recently, we examined stage-specific GM asymmetries in HD based on longitudinal data from the TrackHD project [Tabrizi et al., 2009, 2011, 2012, 2013]. Consistent with the present meta-analysis, we found left-lateralized GM striatal asymmetry in manifest HD, but not at the pre-manifest stage [Minkova et al., Submitted].

Parkinson's Disease

No significant differences in reduced GM or asymmetries in GM decline were found in PD patients relative to controls, even when separating individuals with and without cognitive complaints. We argue that the lack of

significant results in our meta-analysis was driven by the heterogeneity associated with PD. Specifically, PD patients with MCI have previously shown a unilateral GM reduction, including the left superior temporal lobe, left insula, and left superior frontal lobe, compared to those with dementia [Xu et al., 2016]. Another possible explanation could be that studies reporting VBM results in PD did not take into account the side of motor onset, which may result in different patterns of asymmetries mirroring the asymmetric symptomatology. In other words, the lack of GM asymmetries reported here might be caused by individual clinical laterality of PD, which we were unable to account for in the present meta-analysis due to missing meta-data. To our knowledge, only one study has so far addressed this issue [Lee et al., 2015], showing that individuals with left-side motor symptoms had lateralized GM decline predominantly in the right, contralateral hemisphere and performed worse on visuospatial memory tasks than did PD patients with right-side motor symptoms.

Of note, a number of initially identified articles ($n = 20$) in PD were excluded during the literature selection process due to the lack of significant VBM results reported. These data suggest that the VBM approach might be less sensitive to structural changes in PD. Added to this, peak locations reported in the included publications seemed to be rather heterogeneous and mostly found in the frontal, temporal, and parietal lobes, rather than in subcortical regions as we would have expected (see Fig. 3, as well as Supporting Information Fig. S1). Thus, this would have led to the difficulty of finding representative structural changes in PD consistently reported across the studies.

Potential Implications and Future Directions

In light of our meta-analysis, we argue that GM decline occurs asymmetrically but without a clear left-hemisphere preference, selectively targeting brain regions across different neurodegenerative diseases.

In the last decade, a conceptual shift has occurred toward using network-based, rather than region-based, approaches to characterize neurodegenerative diseases [Fornito et al., 2015; Seeley et al., 2009; Zhou et al., 2012]. While there are mostly functional studies, attempts to link functional and structural data indicate that enhanced functional connectivity precedes neurodegeneration at the same location, supporting the assumption of excitotoxic processes as potential mechanisms for neurodegeneration [for a review, see Pievani et al., 2014]. Our findings indicate that studies linking functional and structural (e.g., using fiber tracking) connectivity should add not only GM asymmetry but also its asymmetric distribution.

Naturally, our findings raise the question of how these changes in asymmetries relate to differences observed in clinical manifestation. Mechanisms underlying network abnormalities in neurodegeneration may involve a combination of factors [for a detailed discussion, see Zhou et al., 2012]. These include nodal stress, targeting regions (so-called "hubs") that are subject to heavy network traffic and thus more vulnerable to insult due to excitotoxicity owing to hyperexcitability and metabolic stress [Alstott et al., 2009; Crossley et al., 2014; de Haan et al., 2012]. Another mechanism may involve the transneuronal spread of a toxic agent (e.g., deposition of amyloid β or hyperphosphorylated tau, as in AD) that propagates along network connections. Network abnormalities may also result from regional disconnection due to cell damage or death, resulting in trophic failure. And finally, regions sharing a common gene or protein expression signature, thus equally susceptible to pathological changes, may be part of the same network [Zhou et al., 2012].

However, structural brain networks tend to be asymmetric in their topological organization, with the left hemisphere significantly more "efficient" (i.e., interconnected) in brain regions related to language and motor functions, whereas the right hemisphere showing an increase in nodal efficiency in regions involved in memory and visuospatial attention [Caeyenberghs and Leemans, 2014]. Given these underlying network asymmetries, pathological mechanisms in neurodegenerative diseases may develop in an asymmetric manner, too. However, only few post-mortem studies have addressed the hemispheric asymmetry in pathology distribution, some reporting no asymmetries [Arnold et al., 1991], while others suggesting selective hemispheric asymmetries ($L > R$) of senile plaques and neurofibrillary tangles (tau) in AD [Moossy et al., 1988; Stefanits et al., 2012]. However, the reported asymmetries were limited to the entorhinal cortex and hippocampus but were not found in other cortical regions such as frontal and temporal cortex and basal nucleus of Meynert [Zubenko et al., 1988], and seemed to diminish with increasing disease severity [Moossy et al., 1989], pointing to their changing patterns during disease progression.

In addition to AD [Ossenkoppele et al., 2016], tau pathologies have also been linked to aging [Scholl et al., 2016] as well as recently to HD and the distribution of the mutated form of the *huntingtin* gene [Gratuze et al., 2016; Vuono et al., 2015]. The advancements in imaging the regional distribution of tau pathology with new positron emission tomography (PET) tracers, such as the (18)F-AV1451, may facilitate future studies investigating the patterns of asymmetries associated with neurodegenerative diseases.

Having demonstrated converging evidence suggesting that GM loss might appear asymmetrically in aging and neurodegeneration (albeit at trend levels), as well as the involvement of targeted regions in known functional networks, we here argue that future research should focus on confirming our results and further examining asymmetries on a network level. Furthermore, our understanding of disease progression would benefit from longitudinal studies, as well as studies combining neuroanatomical and functional alterations with post-mortem histopathological

validation in order to assess the potentially cumulative effects of comorbid pathologies that may explain clinical heterogeneity across individuals. More specifically, histopathological studies may provide a valuable insight into the propagation pattern of pathologies along anatomically connected networks, leading to a better understanding of disease progression and functional outcomes in a number of different neurodegenerative diseases, such as (but not limited to) AD, PD, and HD.

ACKNOWLEDGMENT

The authors declare no conflict of interests. LM was partly funded by CHDI Foundation.

AUTHOR CONTRIBUTIONS

LM has full access to all the data in the study and takes responsibility for the integrity of the data and the accuracy of the analyses. Study concept and design: LM, SE, SK. Acquisition, analysis, or interpretation of data: All authors. Drafting of manuscript: LM, SK. Critical revision of the manuscript for important intellectual content: All authors. Statistical analysis: LM, SE, SK. Administrative, technical, or material support: All authors

REFERENCES

Alstott J, Breakspear M, Hagmann P, Cammoun L, Sporns O (2009): Modeling the impact of lesions in the human brain. PLoS Comput Biol 5:e1000408.

Amieva H, Phillips LH, Della Sala S, Henry JD (2004): Inhibitory functioning in Alzheimer's disease. Brain 127:949–964.

Apostolova LG, Steiner CA, Akopyan GG, Dutton RA, Hayashi KM, Toga AW, Cummings JL, Thompson PM (2007): Three-dimensional gray matter atrophy mapping in mild cognitive impairment and mild Alzheimer disease. Arch Neurol 64: 1489–1495.

Arnold SE, Hyman BT, Flory J, Damasio AR, van Hoesen GW (1991): The topographical and neuroanatomical distribution of neurofibrillary tangles and neuritic plaques in the cerebral cortex of patients with Alzheimer's disease. Cereb Cortex 1: 103–116.

Baird AE, Donnan GA, Austin MC, Hennessy OF, Royle J, McKay W (1999): Asymmetries of cerebral perfusion in a stroke-age population. J Clin Neurosci 6:113–120.

Bzdok D, Langner R, Schilbach L, Jakobs O, Roski C, Caspers S, Laird AR, Fox PT, Zilles K, Eickhoff SB (2013): Characterization of the temporo-parietal junction by combining data-driven parcellation, complementary connectivity analyses, and functional decoding. NeuroImage 81:381–392.

Caeyenberghs K, Leemans A (2014): Hemispheric lateralization of topological organization in structural brain networks. Hum Brain Mapp 35:4944–4957.

Cherbuin N, Reglade-Meslin C, Kumar R, Sachdev P, Anstey KJ (2010): Mild cognitive disorders are associated with different patterns of brain asymmetry than normal aging: The PATH through Life Study. Front Psychiatry 1:1–9.

Chetelat G, Landeau B, Salmon E, Yakushev I, Bahri MA, Mezenge F, Perrotin A, Bastin C, Manrique A, Scheurich A, Scheckenberger M, Desgranges B, Eustache F, Fellgiebel A (2013): Relationships between brain metabolism decrease in normal aging and changes in structural and functional connectivity. NeuroImage 76:167–177.

Cieslik EC, Seidler I, Laird AR, Fox PT, Eickhoff SB (2016): Different involvement of subregions within dorsal premotor and medial frontal cortex for pro- and antisaccades. Neurosci Biobehav Rev 68:256–269.

Colcombe SJ, Erickson KI, Scalf PE, Kim JS, Prakash R, McAuley E, Elavsky S, Marquez DX, Hu L, Kramer AF (2006): Aerobic exercise training increases brain volume in aging humans. J Gerontol A Biol Sci Med Sci 61:1166–1170.

Crossley NA, Mechelli A, Scott J, Carletti F, Fox PT, McGuire P, Bullmore ET (2014): The hubs of the human connectome are generally implicated in the anatomy of brain disorders. Brain 137:2382–2395.

de Haan W, Mott K, van Straaten Elisabeth CW, Scheltens P, Stam CJ (2012): Activity dependent degeneration explains hub vulnerability in Alzheimer's disease. PLoS Comput Biol 8:e1002582.

Derflinger S, Sorg C, Gaser C, Myers N, Arsic M, Kurz A, Zimmer C, Wohlschläger A, Mühlau M (2011): Grey-matter atrophy in Alzheimer's disease is asymmetric but not lateralized. J Alzheimers Dis 25:347–357.

Di X, Rypma B, Biswal BB (2014): Correspondence of executive function related functional and anatomical alterations in aging brain. Prog Neuropsychopharmacol Biol Psychiatry 48:41–50.

Eickhoff SB, Etkin A (2016): Going beyond finding the "lesion": A path for maturation of neuroimaging. Am J Psychiatry 173: 302–303.

Eickhoff SB, Stephan KE, Mohlberg H, Grefkes C, Fink GR, Amunts K, Zilles K (2005): A new SPM toolbox for combining probabilistic cytoarchitectonic maps and functional imaging data. NeuroImage 25:1325–1335.

Eickhoff SB, Heim S, Zilles K, Amunts K (2006): Testing anatomically specified hypotheses in functional imaging using cytoarchitectonic maps. NeuroImage 32:570–582.

Eickhoff SB, Paus T, Caspers S, Grosbras MH, Evans AC, Zilles K, Amunts K (2007): Assignment of functional activations to probabilistic cytoarchitectonic areas revisited. NeuroImage 36: 511–521.

Eickhoff SB, Laird AR, Grefkes C, Wang LE, Zilles K, Fox PT (2009): Coordinate-based activation likelihood estimation meta-analysis of neuroimaging data: A random-effects approach based on empirical estimates of spatial uncertainty. Hum Brain Mapp 30:2907–2926.

Eickhoff SB, Jbabdi S, Caspers S, Laird AR, Fox PT, Zilles K, Behrens TEJ (2010): Anatomical and functional connectivity of cytoarchitectonic areas within the human parietal operculum. J Neurosci 30:6409–6421.

Eickhoff SB, Bzdok D, Laird AR, Roski C, Caspers S, Zilles K, Fox PT (2011): Co-activation patterns distinguish cortical modules, their connectivity and functional differentiation. NeuroImage 57:938–949.

Eickhoff SB, Bzdok D, Laird AR, Kurth F, Fox PT (2012): Activation likelihood estimation meta-analysis revisited. NeuroImage 59:2349–2361.

Eickhoff SB, Nichols TE, Laird AR, Hoffstaedter F, Amunts K, Fox PT, Bzdok D, Eickhoff CR (2016): Behavior, sensitivity, and power of activation likelihood estimation characterized by massive empirical simulation. NeuroImage 137:70–85.

Fornito A, Zalesky A, Breakspear M (2015): The connectomics of brain disorders. Nat Rev Neurosci 16:159–172.

Fox PT, Lancaster JL (2002): Opinion: Mapping context and content: The BrainMap model. Nat Rev Neurosci 3:319–321.

Fox PT, Laird AR, Fox SP, Fox PM, Uecker AM, Crank M, Koenig SF, Lancaster JL (2005): BrainMap taxonomy of experimental design: Description and evaluation. Hum Brain Mapp 25: 185–198.

Fox PT, Lancaster JL, Laird AR, Eickhoff SB (2014): Meta-analysis in human neuroimaging: computational modeling of large-scale databases. Annu Rev Neurosci 37:409–434.

Frings L, Hellwig S, Spehl TS, Bormann T, Buchert R, Vach W, Minkova L, Heimbach B, Klöppel S, Meyer PT (2015): Asymmetries of amyloid-beta burden and neuronal dysfunction are positively correlated in Alzheimer's disease. Brain 138:3089–3099.

Giffard B, Laisney M, Mezenge F, de la Sayette V, Eustache F, Desgranges B (2008): The neural substrates of semantic memory deficits in early Alzheimer's disease: Clues from semantic priming effects and FDG-PET. Neuropsychologia 46:1657–1666.

Genon S, Li H, Fan L, Muller VI, Cieslik EC, Hoffstaedter F, Reid AT, Langner R, Grefkes C, Fox PT, Moebus S, Caspers S, Amunts K, Jiang T, Eickhoff SB (2017): The right dorsal premotor mosaic: Organization, functions, and connectivity. Cereb Cortex 27:2095–2110.

Good CD, Johnsrude I, Ashburner J, Henson R, Friston KJ, Frackowiak RS (2001): Cerebral asymmetry and the effects of sex and handedness on brain structure: a voxel-based morphometric analysis of 465 normal adult human brains. NeuroImage 14:685–700.

Goodkind M, Eickhoff SB, Oathes DJ, Jiang Y, Chang A, Jones-Hagata LB, Ortega BN, Zaiko YV, Roach EL, Korgaonkar MS, Grieve SM, Galatzer-Levy I, Fox PT, Etkin A (2015): Identification of a common neurobiological substrate for mental illness. JAMA Psychiatry 72:305–315.

Grady C (2012): The cognitive neuroscience of ageing. Nat Rev Neurosci 13:491–505.

Gratuze M, Cisbani G, Cicchetti F, Planel E (2016): Is Huntington's disease a tauopathy? Brain 139:1014–1025.

Grieve SM, Clark CR, Williams LM, Peduto AJ, Gordon E (2005): Preservation of limbic and paralimbic structures in aging. Hum Brain Mapp 25:391–401.

Henley SMD, Novak MJU, Frost C, King J, Tabrizi SJ, Warren JD (2012): Emotion recognition in Huntington's disease: A systematic review. Neurosci Biobehav Rev 36:237–253.

Hodges JR (2006): Alzheimer's centennial legacy: Origins, landmarks and the current status of knowledge concerning cognitive aspects. Brain 129:2811–2822.

Jagust W (2009): Amyloid + activation = Alzheimer's? Neuron 63: 141–143.

Klöppel S, Draganski B, Siebner HR, Tabrizi SJ, Weiller C, Frackowiak RSJ (2009): Functional compensation of motor function in presymptomatic Huntington's disease. Brain 132:1624–1632.

Kurth F, Gaser C, Luders E (2015): A 12-step user guide for analyzing voxel-wise gray matter asymmetries in statistical parametric mapping (SPM). Nat Protoc 10:293–304.

Laird AR, Fox PM, Price CJ, Glahn DC, Uecker AM, Lancaster JL, Turkeltaub PE, Kochunov P, Fox PT (2005a): ALE meta-analysis: Controlling the false discovery rate and performing statistical contrasts. Hum Brain Mapp 25:155–164.

Laird AR, Lancaster JL, Fox PT (2005b): BrainMap: The social evolution of a human brain mapping database. Neuroinformatics 3:65–78.

Laird AR, Eickhoff SB, Kurth F, Fox PM, Uecker AM, Turner JA, Robinson JL, Lancaster JL, Fox PT (2009): ALE meta-analysis workflows via the Brainmap database: Progress towards a probabilistic functional brain atlas. Front Neuroinform 3:23.

Laird AR, Robinson JL, McMillan KM, Tordesillas-Gutiérrez D, Moran ST, Gonzales SM, Ray KL, Franklin C, Glahn DC, Fox PT, Lancaster JL (2010): Comparison of the disparity between Talairach and MNI coordinates in functional neuroimaging data: Validation of the Lancaster transform. NeuroImage 51: 677–683.

Laird AR, Eickhoff SB, Fox PM, Uecker AM, Ray KL, Saenz JJ Jr, McKay DR, Bzdok D, Laird RW, Robinson JL, Turner JA, Turkeltaub PE, Lancaster JL, Fox PT (2011): The BrainMap strategy for standardization, sharing, and meta-analysis of neuroimaging data. BMC Res Notes 4:349.

Lambrecq V, Langbour N, Guehl D, Bioulac B, Burbaud P, Rotge JY (2013): Evolution of brain gray matter loss in Huntington's disease: A meta-analysis. Eur J Neurol 20:315–321.

Lancaster JL, Tordesillas-Gutiérrez D, Martinez M, Salinas F, Evans A, Zilles K, Mazziotta JC, Fox PT (2007): Bias between MNI and Talairach coordinates analyzed using the ICBM-152 brain template. Hum Brain Mapp 28:1194–1205.

Lancaster JL, Laird AR, Eickhoff SB, Martinez MJ, Fox PM, Fox PT (2012): Automated regional behavioral analysis for human brain images. Front Neuroinform 6:23.

Lee EY, Sen S, Eslinger PJ, Wagner D, Kong L, Lewis MM, Du G, Huang X (2015): Side of motor onset is associated with hemisphere-specific memory decline and lateralized gray matter loss in Parkinson's disease. Parkinsonism Relat Disord 21:465–470.

Long X, Zhang L, Liao W, Jiang C, Qiu B (2013): Distinct laterality alterations distinguish mild cognitive impairment and Alzheimer's disease from healthy aging: Statistical parametric mapping with high resolution MRI. Hum Brain Mapp 34:3400–3410.

Minkova L, Scahill RI, Abdulkadir A, Kaller CP, Peter J, Long JD, Stout JC, Reilmann R, Roos RA, Durr A, Leavitt BR, Tabrizi SJ, Klöppel S. Cross-sectional and longitudinal voxel-based grey matter asymmetries in Huntington's disease. (Submitted)

Moher D, Liberati A, Tetzlaff J, Altman DG (2009): Preferred reporting items for systematic reviews and meta-analyses: The PRISMA statement. J Clin Epidemiol 62:1006–1012.

Moossy J, Zubenko GS, Martinez AJ, Rao GR (1988): Bilateral symmetry of morphologic lesions in Alzheimer's disease. Arch Neurol 45:251–254.

Moossy J, Zubenko GS, Martinez AJ, Rao GR, Kopp U, Hanin I (1989): Lateralization of brain morphologic and cholinergic abnormalities in Alzheimer's disease. Arch Neurol 46:639–642.

Mühlau M, Gaser C, Wohlschläger AM, Weindl A, Städtler M, Valet M, Zimmer C, Kassubek J, Peinemann A (2007): Striatal gray matter loss in Huntington's disease is leftward biased. Mov Disord 22:1169–1173.

Nachev P, Kennard C, Husain M (2008): Functional role of the supplementary and pre-supplementary motor areas. Nat Rev Neurosci 9:856–869.

Ossenkoppele R, Schonhaut DR, Scholl M, Lockhart SN, Ayakta N, Baker SL, O'Neil JP, Janabi M, Lazaris A, Cantwell A, Vogel J, Santos M, Miller ZA, Bettcher BM, Vossel KA, Kramer JH, Gorno-Tempini ML, Miller BL, Jagust WJ, Rabinovici GD (2016): Tau PET patterns mirror clinical and neuroanatomical variability in Alzheimer's disease. Brain 139:1551–1567.

Pievani M, Filippini N, van den Heuvel MP, Cappa SF, Frisoni GB (2014): Brain connectivity in neurodegenerative diseases—from phenotype to proteinopathy. Nat Rev Neurol 10:620–633.

Raz N, Gunning FM, Head D, Dupuis JH, McQuain J, Briggs SD, Loken WJ, Thornton AE, Acker JD (1997): Selective aging of the human cerebral cortex observed in vivo: Differential vulnerability of the prefrontal gray matter. Cereb Cortex 7: 268–282.

Salimi-Khorshidi G, Smith SM, Keltner JR, Wager TD, Nichols TE (2009): Meta-analysis of neuroimaging data: A comparison of image-based and coordinate-based pooling of studies. NeuroImage 45:810–823.

Scholl M, Lockhart SN, Schonhaut DR, O'Neil JP, Janabi M, Ossenkoppele R, Baker SL, Vogel JW, Faria J, Schwimmer HD, Rabinovici GD, Jagust WJ (2016): PET imaging of tau deposition in the aging human brain. Neuron 89:971–982.

Seeley WW, Menon V, Schatzberg AF, Keller J, Glover GH, Kenna H, Reiss AL, Greicius MD (2007): Dissociable intrinsic connectivity networks for salience processing and executive control. J Neurosci 27:2349–2356.

Seeley WW, Crawford RK, Zhou J, Miller BL, Greicius MD (2009): Neurodegenerative diseases target large-scale human brain networks. Neuron 62:42–52.

Shattuck DW, Mirza M, Adisetiyo V, Hojatkashani C, Salamon G, Narr KL, Poldrack RA, Bilder RM, Toga AW (2008): Construction of a 3D probabilistic atlas of human cortical structures. NeuroImage 39:1064–1080.

Smith SM, Fox PT, Miller KL, Glahn DC, Fox PM, Mackay CE, Filippini N, Watkins KE, Toro R, Laird AR, Beckmann CF (2009): Correspondence of the brain's functional architecture during activation and rest. Proc Nat Acad Sci USA 106: 13040–13045.

Stefanits H, Budka H, Kovacs GG (2012): Asymmetry of neurodegenerative disease-related pathologies: A cautionary note. Acta Neuropathol 123:449–452.

Tabrizi SJ, Langbehn DR, Leavitt BR, Roos RA, Durr A, Craufurd D, Kennard C, Hicks SL, Fox NC, Scahill RI, Borowsky B, Tobin AJ, Rosas HD, Johnson H, Reilmann R, Landwehrmeyer B, Stout JC (2009): Biological and clinical manifestations of Huntington's disease in the longitudinal TRACK-HD study: Cross-sectional analysis of baseline data. Lancet Neurol 8: 791–801.

Tabrizi SJ, Scahill RI, Durr A, Roos RA, Leavitt BR, Jones R, Landwehrmeyer GB, Fox NC, Johnson H, Hicks SL, Kennard C, Craufurd D, Frost C, Langbehn DR, Reilmann R, Stout JC (2011): Biological and clinical changes in premanifest and early stage Huntington's disease in the TRACK-HD study: The 12-month longitudinal analysis. Lancet Neurol 10:31–42.

Tabrizi SJ, Reilmann R, Roos RA, Durr A, Leavitt BR, Owen G, Jones R, Johnson H, Craufurd D, Hicks SL, Kennard C, Landwehrmeyer B, Stout JC, Borowsky B, Scahill RI, Frost C, Langbehn DR (2012): Potential endpoints for clinical trials in premanifest and early Huntington's disease in the TRACK-HD study: Analysis of 24 month observational data. Lancet Neurol 11:42–53.

Tabrizi SJ, Scahill RI, Owen G, Durr A, Leavitt BR, Roos RA, Borowsky B, Landwehrmeyer B, Frost C, Johnson H, Craufurd D, Reilmann R, Stout JC, Langbehn DR (2013): Predictors of phenotypic progression and disease onset in premanifest and early-stage Huntington's disease in the TRACK-HD study: Analysis of 36-month observational data. Lancet Neurol 12: 637–649.

Thompson PM, Mega MS, Woods RP, Zoumalan CI, Lindshield CJ, Blanton RE, Moussai J, Holmes CJ, Cummings JL, Toga AW (2001): Cortical change in Alzheimer's disease detected with a disease-specific population-based brain atlas. Cereb Cortex 11:1–16.

Thompson PM, Hayashi KM, de Zubicaray G, Janke AL, Rose SE, Semple J, Herman D, Hong MS, Dittmer SS, Doddrell DM, Toga AW (2003): Dynamics of gray matter loss in Alzheimer's disease. J Neurosci 23:994–1005.

Thompson PM, Hayashi KM, Dutton RA, Chiang MC, Leow AD, Sowell ER, De Zubicaray G, Becker JT, Lopez OL, Aizenstein HJ, Toga AW (2007): Tracking Alzheimer's disease. Ann NY Acad Sci 1097:183–214.

Toga AW, Thompson PM (2003): Mapping brain asymmetry. Nat Rev Neurosci 4:37–48.

Turkeltaub PE, Eden GF, Jones KM, Zeffiro TA (2002): Meta-analysis of the functional neuroanatomy of single-word reading: Method and validation. NeuroImage 16:765–780.

Turner JA, Laird AR (2012): The cognitive paradigm ontology: Design and application. Neuroinformatics 10:57–66.

Vuono R, Winder-Rhodes S, de Silva R, Cisbani G, Drouin-Ouellet J, Spillantini MG, Cicchetti F, Barker RA (2015): The role of tau in the pathological process and clinical expression of Huntington's disease. Brain 138:1907–1918.

World Medical Association (2013): World Medical Association Declaration of Helsinki. JAMA 310:2191.

Xu Y, Yang J, Hu X, Shang H (2016): Voxel-based meta-analysis of gray matter volume reductions associated with cognitive impairment in Parkinson's disease. J Neurol 263:1178–1187.

Zhou J, Gennatas ED, Kramer JH, Miller BL, Seeley WW (2012): Predicting regional neurodegeneration from the healthy brain functional connectome. Neuron 73:1216–1227.

Zubenko GS, Moossy J, Hanin I, Martinez AJ, Rao GR, Kopp U (1988): Bilateral symmetry of cholinergic deficits in Alzheimer's disease. Arch Neurol 45:255–259.